Short Communication

Quantitative description of yttrium aluminate ceramic composition by means of Er^{+3} microluminescence spectrum

F.A. Videla [a, b], M.R. Tejerina [b, c, *], L. Moreira-Osorio [d], M.S. Conconi [c], D.J.O. Orzi [a], T. Flores [d], L.V. Ponce [d], G.M. Bilmes [a, b], G.A. Torchia [a]

[a] Centro de Investigaciones Ópticas (CONICET La Plata-CIC-UNLP), CC n° 3, M.B. Gonnet (1897), Buenos Aires, Argentina
[b] Facultad de Ingeniería, Universidad Nacional de La Plata, Av. 1 750 (1900), La Plata, Buenos Aires, Argentina
[c] Centro de Tecnología de Recursos Minerales y Cerámica (CONICET La Plata-CIC), CC n° 49, M.B. Gonnet (1897), Buenos Aires, Argentina
[d] Tecnología Láser, IPN, CICATA-Unidad Altamira, Km 14.5, Carretera Tampico-Puerto Industrial Altamira, Altamira, Tamaulipas C.P. 89600, Mexico

ARTICLE INFO

ABSTRACT

The composition of erbium-doped yttrium aluminate ceramics was analyzed by means of confocal luminescence spectroscopy, EDX, and X-ray diffraction. A well-defined linear correlation was found between a proposed estimator computed from the luminescence spectrum and the proportion of ceramic phases coexisting in different samples. This result shows the feasibility of using erbium luminescence spectroscopy to perform a quantitative determination of different phases of yttrium aluminates within a micrometric region in nanograined ceramics.

© 2018 Elsevier B.V. All rights reserved.

Yttrium aluminum garnet and perovskite (YAG and YAP) are relevant host materials for solid-state lasers, solid-state-lighting phosphors, scinterizations, active photonic waveguides, optical lenses and thermal coating manufacturing [1–5]. In this sense, the manufacturing processes, crystalline structure and spectroscopic properties of these ceramics doped with rare earth ions, among other characteristics, have been studied from the 1970s up to now [5–14].

A relevant characteristic of any ceramic sample is the determination of the phases present and their percentage either in bulk material or in a micrometric region, depending on the specific application of the material. To determine the different phases present in a compound, generally, the most commonly employed technique is X-ray diffraction (XRD). This is a well-known technique that allows a quantitative but macroscopic estimation of the percentage of different phases present in the material by means of Rietveld refinement technique [15].

In this work, we propose a method that employs luminescence spectroscopy to determine the composition of homemade erbium-doped yttrium aluminate ceramics. The obtained result was compared with the well-established XRD Rietveld refinement

technique. Although the method presented herein requires that a dopant ion replaces an atom of each analyzed phase, the determination of phases by luminescence spectroscopy has some advantages. The samples do not need any special preparation. This spectroscopy can be performed by an instantaneous measurement, and also simultaneously with other processes, for example, during annealing [16,17]. Furthermore, taking into account recently advances in photonic structures and the emergence of nanograined ceramics, it has become necessary to determine, within microscopic regions, the different phases that compose the solid and their spatial distribution [18,19]. The luminescence emission spectrum is a valid option for this particular target. In this sense, a commercial confocal luminescence microscope with motorized stages allows a luminescence map analysis of several micrometer-sized regions with spatial steps of about 0.5 μm minimum [3,20].

The studied ceramic samples were manufactured using the dry method or mechanochemical synthesis. The starting materials were: α-Al_2O_3 (125 nm of particle size) and Y_2O_3 (1115 nm of particle size) from Baikowski Japan; and Er_2O_3 (50 nm of particle size), tetraethyl orthosilicate (TEOS) and ethanol from Sigma-Aldrich. Every component had a purity higher than 99.99% with the exception of ethanol, which had a purity of 99.95%. At first, aluminum oxides, yttrium and erbium were mixed in a stoichiometric proportion of 2.0 at% Er:YAG. The sintering additive, TEOS as SiO_2 source, was added to the mentioned set of oxides. The mixture was milled in a ball mill using alumina balls of high purity and

* Corresponding author. Facultad de Ingeniería, Universidad Nacional de La Plata, La Plata, Buenos Aires, Argentina.
E-mail address: matiast@cetmic.unlp.edu.ar (M.R. Tejerina).

10 mm diameter, using ethanol as solvent. After grinding, the samples were dried at 100 °C for 24 h and subsequently sieved using frames with 200 mesh, 250 mesh and 325 mesh. The powders obtained were sintered at 600 °C for 6 h to remove all kinds of organic components present. Subsequently, the green compact body was formed, where the mix of powders was uniaxially pressed at 350 MPa for 10 min. Finally the green body was sintered in vacuum (10^{-7}) without applying additional external pressure, at temperatures between 1450 °C and 1550 °C for 12 h [2]. In Table 1, a description of the different characteristics of the studied ceramic samples is presented. As expected [2], the obtained ceramic samples were not optically transparent.

S0 sample was an Er:YAG crystal from Baikowski Japan highly doped with 50% mass ratio of rare earth concentration. The different surfaces of the samples were polished with various sizes of diamond powders up to optical quality (1/4 μm) to improve the luminescence signal and the response of surface analysis. In the surface of all the samples, a standard deposition of Carbon (C) was performed to allow SEM and EDX measurements.

The system employed to collect the luminescence spectra was a HORIBA Xplora PLUS Confocal Raman Microscope. It consists of an OLYMPUS microscope BX-41, a computer-assisted translation stage with a resolution of 0.5 μm and laser sources of 785 and 532 nm, different gratings (600, 1200, 1800 and 2400 gr/mm) and a HORIBA CCD refrigerated at −60 °C. The typical spectral resolution of the system is 0.5 cm^{-1}.

A SEM FEI Quanta200 electron microscope was used to inspect the micro- and nanostructure. This instrument has CCD detectors and reaches 3.0 nm and 10 nm of resolution at 10 kV and 3 kV respectively. The accelerating voltage can be ranged from 200 V to 30 kV. A JEOL JCM-6000 was employed to measure EDX signals and to take backscattered electrons intensity (BEI) images. To perform XRD measurements, a Bruker XRD D2 Phaser was used.

To study the topography of samples, an atomic force microscope provided by VEECO was employed. It comprises a V control unit and a multimode microscope. The measurements were performed in "tapping" mode employing a silicon nitride tip with an oscillation frequency of 300 KHz and a cantilever spring constant of 40 N/m. The cantilever deflection was detected with a TAO 3000 DLC budget sensor.

At first, to analyze grain morphology and pores size, we scanned the ceramic surface of the different samples with atomic force microscopy (AFM). Fig. 1(a) shows an AFM height profile of sample S3 surface; similar images were obtained for S1 and S2. Subregions with a characteristic length of some microns, undefined limits and irregular shape and pores of at least 1500 nm depth can be observed. The ratio between holes (denoted by dark regions) and

plane areas was analyzed using AFM processing software, and it was concluded that it was around $14 \pm 2\%$. This elevated porosity makes ceramic samples opaque [21,22]. A roughness mean value of 2 ± 0.5 nm was determined in the surface of polished faces. It was not possible to observe grain boundaries employing the AFM technique. In Fig. 1(b), a SEM image of sample S3 is shown, being similar to those obtained for S1 and S2. By means of this technique, it was found that the subregions shown in Fig. 1(a) are composed of submicrometer-sized grains. Crystalline grains are several nanometers in size and are grouped in regions of micrometric volume with undefined boundaries. Therefore, the different phases coexisting in the material can be grouped in micrometric or smaller regions.
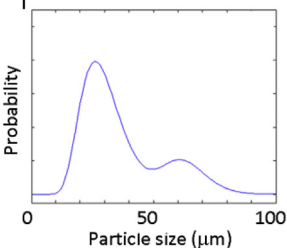
To identify and quantify the different crystalline phases coexisting in the studied samples, we performed XRD analysis. The XRD patterns for each sample are shown in Fig. 2. All the samples had a high percentage of garnet phase ($Al_5Y_3O_{12}$); however, a minor percentage of perovskite ($YAlO_3$) was also found. The proportion for each crystalline phase obtained by Rietveld refinement is listed in Table 2. The obtained refinement statistical indicator Rwp has acceptable values and is also shown in this table. It is observed that the amount of perovskite and other secondary crystalline phases (diaspore AlO(OH) and alumina oxide αAl_2O_3) decreased when the sintering temperature increased. This is an expected behavior according to previously published work [23,24]. Therefore, sample S3 is almost fully composed of garnet structured grains. Diaspore hydroxide should not resist calcinations but it could be generated after sintering if the oxide surface was highly reactive when the samples were exposed to an open atmosphere.

Regarding all the phases detected by XRD and quantified by Rietveld method, the variation in the composition between the different ceramic samples resulted minor than 2%. About a 55% of oxygen atoms, a 26% of aluminum atoms and a 14% of yttrium plus erbium was computed. To analyze the average chemical composition of samples, an EDX spectrum in a region of 60×60 μm^2 was performed in each sample surface. According to this, the composition quantified for all the samples (S0,S1,S2,S3) agreed between them, and these agreed with that computed by using the phases detected by XRD, within an uncertainty of 3% (in mass percentage). As expected, in the case of crystalline sample around a 10% of erbium atom was found, this is a high percentage in comparison with that found in ceramic samples, below of 1%. To make it possible a comparison between the chemical composition of crystalline and ceramic samples, erbium atoms concentration was summed to yttrium concentration because erbium replace yttrium in garnet crystalline structure.

To analyze the spatial distribution of the different phases, a

Table 1
Manufacture characteristics of the studied ceramic samples. Bimodal distribution of powder sizes, standard deviation and time and temperatures used during their sintering. Percentages of additives used for sintering are also indicated.

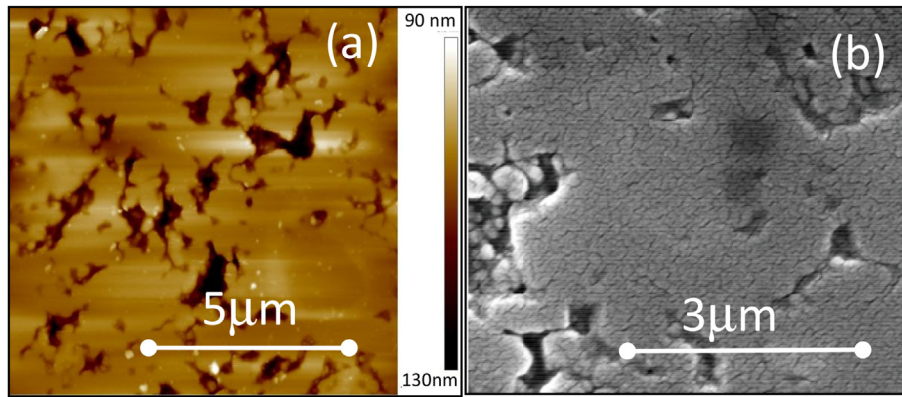| Sample	Starting Composition	Size Powder Distribution 1	GSD (Powder)	σ(μm) (Powder)	Temperature (°C)	Time (h)
S1	$(0.06Er_2O_3 + 2.94\,Y_2O_3 + 5Al_2O_3) + 0.25$ wt%$SiO_2 + 0.25$ wt%B_2O_3		1.35	30.16	1450	12
S2					1500	
S3					1550	

Fig. 1. (a) AFM image of S3 sample (b) SEM image of S2 sample (20 Kv).
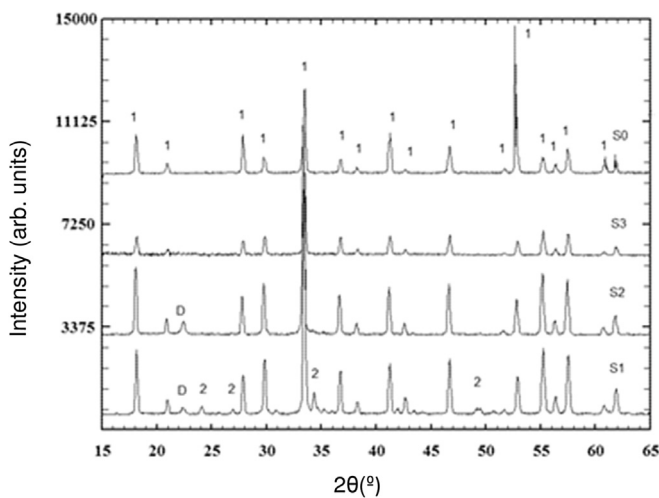

Fig. 2. XRD patterns of a manufactured ceramic and commercial crystalline sample (after milling). Peaks corresponding to garnet and perovskite phase are labeled with "1" and "2", respectively. Those corresponding to diaspore are labeled with "D".

backscattered electrons image was performed on the surface of each ceramic sample and is presented in Fig. 3. In this kind of image, the degree of intensity is an indicator of the average atomic number of irradiated composites. After a detailed exploration of the different regions employing EDX technique in each ceramic sample, it was concluded that:

- the majoritarian gray phase is $Y_3Al_5O_{12}$ with low concentration of erbium ions (<1%). This phase has a mean atomic number of 13.9 and is labeled as R1 in Fig. 3.
- the dark regions are mainly composed by α-Al_2O_3 or AlO(OH) (labeled as R2). These phases have a mean atomic number between 7.5 and 10.
- the light gray regions (labeled as R3) are composed by $YAlO_3$ with low concentration of erbium ions (<1%). This phase has a

mean atomic number of 15.2, and as expected, is only observed in S1 and S2.
- the brighten regions (labeled as R4) are composed by Er:$YAlO_3$ and Er:$YAlO_3$ with different proportions of high Er-doping (between 24 and 60% in mass). The mean atomic number of this group of phases is between 16 and 21.

An EDX spectrum within each region (R1, R2, R3 and R4) and the result of semi-quantitative analysis with ZAF method [25] are presented in Fig. 3(b). There, atom ratio of the different phases can be observed. Erbium percentage is less than 1% in regions R1 and R3, so it is not detected with the employed integration times. Regarding the composition of the different regions, we can mention the following. Within R2 spectrum, only aluminum and oxygen are detected according with AlO3 and Al(OH) composition; for R1, Al/Y ratio in atom percentage is about "2", which is near to "1.6", the Al/Y ratio for YAG($Y_3Al_5O_{12}$); for region R3 this ratio is about 0.7, which is near to "1" the Al/Y ratio of YAP ($YAlO3$). In R4 composition, it can be found a high concentration of erbium and this value considerably varied in different measurements, because erbium can replace one, two or three sites in YAG and an average signal of different combinations of them can be detected. In Table 3 we present a comparison between measured composition in mass and theoretical one. There it can be seen that composition, in general, agreed with theoretical values.

By taking into account DRX results, the ceramic samples have different amounts of YAG and YAP phases, so we studied their emission spectra in the range of $^4S_{3/2}$->$^4I_{15/2}$ transitions, from 536 to 563 nm, and performed a first qualitatively comparison between the spectrum of each ceramic sample and the well-known luminescence spectrum of the Er:YAG commercial crystalline sample, which is shown in Fig. 4. It can be seen that with increasing sintering temperature, the spectrum of the ceramic becomes almost equal to that of crystalline Er:YAG. As is known, the Er$^+$ luminescence spectrum of a high quality garnet ceramic should not be different from the crystalline garnet YAG sample spectrum [18]. Relevant peaks belonging to the emission of erbium ions inside the YAP structure were identified and labeled in Fig. 4 according to a previously published work [26]. It is clear that the intensity of these

Table 2
Phase composition in volume obtained from Rietveld refinement.

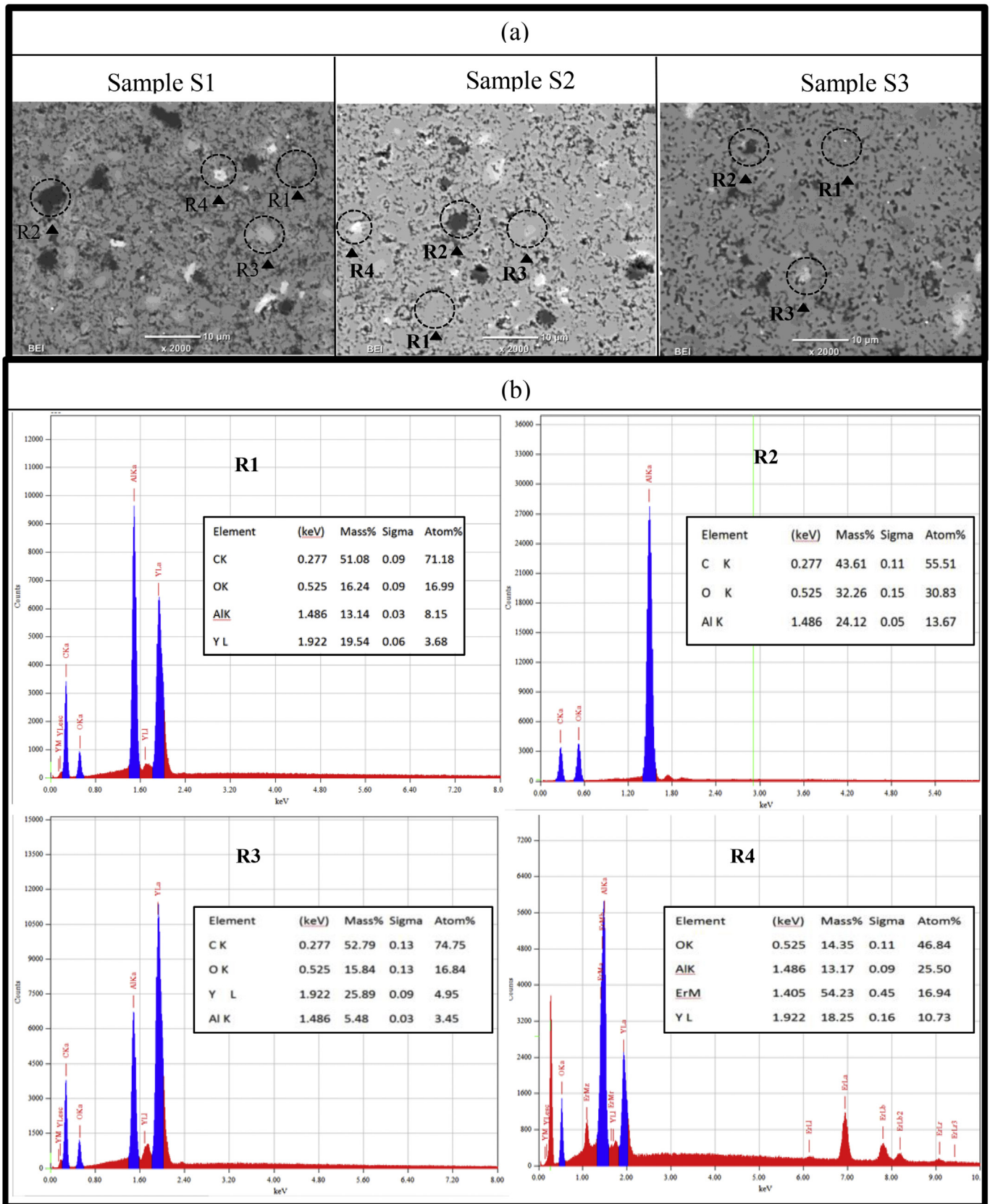| Sample	$Al_5Y_3O_{12}$ garnet (1)	Y AlO_3 perovskite (2)	αAl_2O_3	Diaspore AlO(OH) (D)	Rwp
S0	99.5 (0.2)	–	–	–	25.2
S1	79.2 (0.2)	9.4 (0.2)	3.40 (0.07)	7.9 (0.1)	15.6
S2	90.1 (0.2)	1.98 (0.09)	1.74 (0.07)	5.9 (0.2)	17.3
S3	98.2 (0.2)	<1%	–	<1%	18.3

Fig. 3. (a) Back scattered electrons intensity from surface of ceramic samples (b) atomic composition of detected phases for the different ceramic samples.

Table 3
Comparison between retrieved composition and theoretical one in mass percetage. For EDX semi-quantitative analysis an uncertainty of 5 % is estimated.

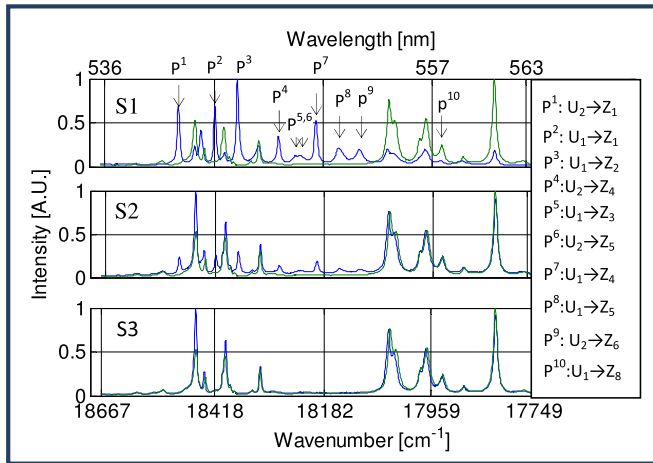| Phase Atom	EDX	Nominal	EDX	Nominal	EDX	Nominal	EDX	Nominal
	R1	$Y_3Al_5O_{12}$	R2	$Al_2O_3/$ $AlO(OH)$	R3	$YAlO_3$	R4	$Er:Y_3Al_5O_{12}$ $/Er:YAlO_3$
O	33%	44%	57%	47 to 52%	33%	32%	14%	19 to 25%
Al	26%	22%	42%	44 to 52%	11%	22%	13%	11 to 20%
Y	39%	32%	-	-	54%	44%	18%	11 to 44%
Er	-	-	-	-	-	-	54%	44 to 70%

Fig. 4. Comparison between different ceramic emission (blue spectra) and crystalline YAG spectrum (green spectrum). Each YAG or YAP spectrum was normalized at maximum intensity. The lines correspond to the $^4S_{3/2}$ to $^4I_{15/2}$ emission lines (U_x is the energy level and Zy is a stark level). (For interpretation of the references to colour in this figure legend, the reader is referred to the Web version of this article.)

transitions decreases when the YAP phase is reduced. The variation of the luminescence spectrum for the different samples is explained in terms of a structural difference between garnet and perovskite phases that leads to a different surrounding lattice field of the rare earth ion, which modifies the emission spectrum [27]. No shifting of spectral lines was observed between the different ceramic samples, within an uncertainty of 0.3 cm^{-1}.

If we compare the luminescence results to that obtained with XRD analysis, we can see that they are qualitatively similar. However, could a quantitative relation between the mass percentage of the phases present in a sample and its luminescence spectrum be established? To answer this question and evaluate the application of Er^{+3} luminescence spectrum to determine the composition of ceramics, we made the following assumptions.

As the ionic radius of the erbium ion (1.004 Å) is similar to that of yttrium (1.019 Å), it was assumed that erbium ions replace yttrium in the perovskite and garnet structure [28] and other possible contributions of erbium emission from the remaining phases, i.e., aluminate oxide, diaspore and the other amorphous phases, were assumed negligible. Then, we supposed that the measured spectra correspond to the emission of erbium ions inside the perovskite and garnet structure, and that the total measured intensity ($I_i(\lambda)$) is composed of these two different spectra linearly summed, as shown in Equation (1). We did not take into account any interaction between emissions of different phases.

$$I_i(\lambda) = I_{ip}(\lambda) + I_{ig}(\lambda) \qquad (1)$$

where: $I_i(\lambda)$ is the luminescence intensity measured from each sample $i = 1...3$, $I_{ip}(\lambda)$ is the intensity corresponding to perovskite

nanograin signal, and $I_{ig}(\lambda)$ corresponds to garnet nanograin signal.

We measured the Er:YAG luminescence spectrum from crystalline sample S0. This spectrum represents the $I_{ig}(\lambda)$ spectrum, but it was adequately normalized to be subtracted from each $I_i(\lambda)$ spectrum. To carry out this task, the peak at around 560 nm was fitted, which is not allowed for Er^{+3} emission in YAP structure. Then, by subtracting a normalized $I_{ip}(\lambda)$ from each $I_i(\lambda)$, the $I_{ip}(\lambda)$ spectrum component was obtained. Afterward, by assuming that the intensity of each phase spectrum ($I_p(\lambda)$ and $I_g(\lambda)$) is proportional to the volume occupied by each phase, we integrated the intensity of both YAP and YAG spectra, and computed a ratio between them (I_{YAP}/I_{YAG}). To minimize undesirable noise, this procedure was performed in a set of two thousand spectra measured in each ceramic sample (S1, S2 and S3). These measurements were taken in 1000 points within an area of about 2000 μm². The average spectrum over this area is equivalent to a photoluminescence bulk measurement. Finally, we compared the proportion I_{YAP}/I_{YAG} obtained from luminescence spectroscopy with the volume ratio YAP/YAG obtained from the well-known XRD Rietveld refinement method. This comparison is presented in Fig. 5, where it can be seen that the result of the applied procedure has a clear linear correlation with the phase composition obtained by XRD for the different samples, especially for mean values of I_{YAP}/I_{YAG}. The standard deviation of this estimator (I_{YAP}/I_{YAG}) was computed for each sample and is presented as uncertainty bars. A larger dispersion of this parameter was found for sample S2, in comparison with the other
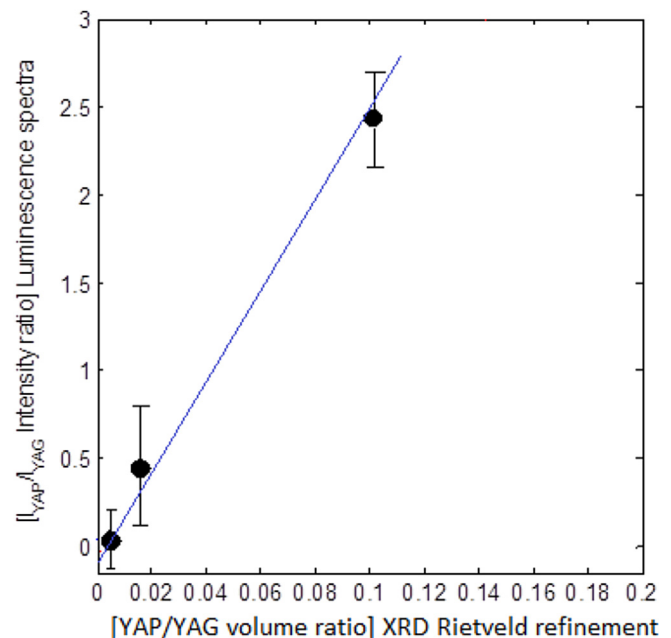

Fig. 5. I_{YAP}/I_{YAG} luminescence spectral intensity ratios vs. YAP/YAG volume ratio obtained from XRD Rietveld refinement.

samples.

In this work, we presented a method to quantitatively determine the composition of yttrium aluminum ceramics by employing luminescence spectroscopy. This method was designed by taking advantage of the fact that the optical transitions of rare earth ions are highly affected by the lattice surrounding the structure of YAP and YAG, so the luminescence spectrum depends on the phase where the erbium ion is located. The good correlation obtained with XRD results indicates that this method can be employed to determine the proportion of YAG and YAP phases present in a ceramic. Also, the detected phases were corroborated by EDX and BEI images. The advantages of determining the composition by luminescence spectroscopy are mentioned at the beginning of this work.

In future work, we will analyze the composition of the studied material in a specific micrometric region of the material surface using luminescence maps combined with EDX maps, which is expected to improve the presented methodology. Furthermore, we will also analyze the scope of luminescence spectroscopy to identify the different phases present in other ceramic materials and determine their composition. To this end, rare earth doping in minimal proportions (below 1%) can be intentionally performed.

Acknowledgements

References

[1] A. Ikesue, I. Furusato, K. Kamata, Fabrication of polycrystalline, transparent YAG ceramics by a solid-state reaction method, J. Am. Ceram. Soc. 78 (1995) 225–228.

[2] L. Moreira, L. Ponce, E. de Posada, T. Flores, Y. Peñaloza, O. Vázquez, Y. Pérez, Er:YAG polycrystalline ceramics: the effects of the particle size distribution on the structural and optical properties, Ceram. Int. 41 (2015) 11786–11792.

[3] R.C. Powell, Miscellaneous laser materials, in: Physics of Solid State Laser Materials, AIP, New York, 1998, pp. 380–416.

[4] T. Jüstel, H. Nikol, C. Ronda, New developments in the field of luminescent materials for lighting and displays, Angew. Chem. Int. Ed. 37 (1998) 3085–3103.

[5] D. Michalik, T. Pawlik, J. Plewa, M. Sopicka-Lizer, Influence of homogenization and micro/nano source of starting powders on format ion of the single YAP phase, Arch. Metall. Mater. 61 (2016) 1753–1760.

[6] M.J. Weber, M. Bass, G.A. deMars, Laser action and spectroscopic properties of Er3+ in YAlO3, J. Appl. Phys. 42 (1971) 301–305.

[7] J. Li, Y. Wu, Y. Pan, W. Liu, L. Huang, J. Guo, Fabrication, microstructure and properties of highly transparent Nd:YAG laser ceramics, Optic. Mater. 31 (2008) 6–17.

[8] M.G. Beghi, C.E. Bottani, V.J. Russo, Debye temperature of erbium-doped yttrium aluminum garnet from luminescence and Brillouin scattering data, Appl. Phys. 87 (2000) 1769–1774.

[9] S. Kaveh, C.P. Tremblay, N. Norhashim, R.J. Curry, A.K. Cheetham, Phase separation in garnet solid solutions and its effect on optical properties, Adv. Mater. 25 (2013) 6448–6452.

[10] N. Nurhakimah, PhD. dissertation, University of Surrey, Surrey, 2017.

[11] J. Zhou, W. Zhang, L. Wang, Y. Shen, J. Li, W. Liu, B. Jiang, H. Kou, Y. Shi, Y. Pan, Fabrication, microstructure and optical properties of polycrystalline Er3+: Y3Al5O12 ceramics, Ceram. Int. 37 (2011) 119–125.

[12] A. Lukowiak, R.J. Wiglusz, M. Maczka, P. Gluchowski, W. Strek, IR and Raman spectroscopy study of YAG nanoceramics, Chem. Phys. Lett. 494 (2010) 279–283.

[13] A. Ikesue, K. Kamata, Microstructure and optical properties of hot isostatically pressed Nd:YAG ceramics, J. Am. Ceram. Soc. 79 (1996) 1927–1933.

[14] Y.H. Zhou, J. Lin, M. Yu, S.M. Han, S.B. Wang, H.J. Zhang, Morphology control and luminescence properties of YAG: Eu phosphors prepared by spray pyrolysis, Mater. Res. Bull. 38 (2003) 1289–1299.

[15] C.T. Kniess, J. Cardoso de Lima, P.B. Prates, The quantification of crystalline phases in materials: applications of Rietveld method, in: V. Shatokha (Ed.), Sintering - Methods and Products, InTech, 2012, pp. 293–316.

[16] L. Niewolak, D. Naumenko, E. Wessel, L. Singheiser, W.J. Quadakkers, Optical fluorescence spectroscopy for identification of minor oxide phases in alumina scales grown on high temperature alloys, Mater. Char. 55 (2005) 320–331.

[17] C. Tsai, K.-H. Li, J. Sarathy, S. Shih, J.C. Campbell, B.K. Hance, J.M. White, Thermal treatment studies of the photoluminescence intensity of porous silicon, Appl. Phys. Lett. 59 (1991) 2814–2816.

[18] A. Rodenas, A. Benayas, J.R. Macdonald, J. Zhang, D.Y. Tang, D. Jaque, A.K. Kar, Direct laser writing of near-IR step-index buried channel waveguides in rare earth doped YAG, Opt. Lett. 36 (2011) 3395–3397.

[19] H.M. Wang, J.S. Jiang, Z.Y. Huang, Y. Chen, K. Liu, Z.W. Lu, J.Q. Qi, F. Li, D.W. He, T.C. Lu, Q.Y. Wang, Determination of the compressive yield strength for nanograined YAG transparent ceramic by XRD analysis, J. Alloys Compd. 671 (2016) 527–531.

[20] M.O. Ramirez, A. Stevenson, J. Stitt, G.L. Messing, V. Gopalan, in: Confocal Micro-Fluorescence and Raman Spectroscopy across Grain Boundaries in Transparent Nd3+:YAG Ceramic Laser Gain Media, Conference Paper in Conference on Lasers and Electro-optics (CLEO), OSA, May 2007, p. CMW4.

[21] Y. Wang, J. Zhang, Y. Zhao, Strength weakening by nanocrystals in ceramic materials, Nano Lett. 7 (2007) 3196–3199.

[22] R.P. Yavetskiy, E.A. Vovk, A.G. Doroshenko, M.I. Danylenko, A.V. Lopin, I.A. Petrusha, V.F. Tkachenko, A.V. Tolmachev, V.Z. Turkevich, Y3Al5O12 translucent nanostructured ceramics—Obtaining and optical properties, Ceram. Int. 37 (2011) 2477–2484.

[23] W. Guo, Y. Cao, Q. Huang, J. Li, J. Huang, Z. Huang, F. Tang, Fabrication and laser behaviors of Nd:YAG ceramic microchips, J. Eur. Ceram. Soc. 31 (2011) 2241–2246.

[24] L. Zych, R. Lach, The effect of powders homogenisation conditions on the synthesis of yttrium aluminium garnet (YAG) by a solid-state reaction, Ceram. Int. 43 (2017) 4029–4036.

[25] L. Reimer, Scanning Electron Microscopy, Springer Series in Optical Sciences, 1998.

[26] D.K. Sardar, S. Chandrasekharan, K.L. Nash, J.B. Gruber, Optical intensity analyses of Er3+:YAlO3, J. Appl. Phys. 104 (2008), 023102.

[27] M. Jelinek, J. Oswald, V. Studnicka, J. Lancok, M. Pavelka, D. Chvostova, V. Slechtova, K. Nejezchleb, A. Mackova, C. Grivas, in: Optical Properties of Er: YAG and Er:YAP Materials and Layers Grown by Laser, Conference Paper in Photonics, Devices, and Systems II, SPIE, July 2003, p. 268.

[28] L. Dobrzycki, E. Bulska, D.A. Pawlak, Z. Frukacz, K. Woźniak, Structure of YAG crystals doped/substituted with erbium and ytterbium, Inorg. Chem. 43 (2004) 7656–7664.